

## Fabrication of thermal barrier coatings on the inner surface of carbon steel tubular components via a novel mechanical alloying method

Bo Li<sup>1, a</sup>, Yifu Shen<sup>2, b</sup>

<sup>1</sup>Shanghai Institute of Special Equipment Inspection and Technical Research, 399 North Nuijiang Road, Shanghai 200333, PR China

<sup>2</sup>College of Materials Science and Technology, Nanjing University of Aeronautics and Astronautics, 29 Jiangjun Road, Nanjing 210016, PR China

<sup>a</sup>libo@ssei.cn, <sup>b</sup>yifushen\_nuaa@hotmail.com

**Keywords:** Mechanical alloying; Thermal barrier coating; Tubular component; Surface; Oxidation

**Abstract.** The thermal barrier coatings of  $\text{NiCrAl}\cdot\text{Y}_2\text{O}_3$  and  $\text{NiCrAlCo}\cdot\text{Y}_2\text{O}_3$  were fabricated on the inner surface of low carbon steel tubular components via a novel high-energy mechanical alloying method. The microstructure, elemental distribution and phase composition of the prepared coatings were carefully investigated by the X-ray diffraction analyzer, scanning electron microscope and energy dispersive X-ray spectroscopy. The thermal oxidation experiments were performed to inspect the anti-oxidation properties of the coatings. The addition of Co element contributed to the resistance against the thermal oxidation, comparing to that of the  $\text{NiCrAl}\cdot\text{Y}_2\text{O}_3$  coatings and the bare substrate. The anti-oxidation mechanism of  $\text{NiCrAlCo}\cdot\text{Y}_2\text{O}_3$  coatings was discussed in the paper. The thermal barrier function of the coatings was greatly useful for carbon steel tubes or pipes. In addition, the thermal barrier coating fabrication method indicated more efficient and productive than many other processing methods for obtaining functional coatings. According to the analyses of the experimental results, the formation mechanisms of the deposited coatings prepared by mechanical alloying method were detailed in terms of three assumed but reasonable steps.

### Introduction

Improvement in efficiencies of gas turbines can be achieved by increasing the gas inlet turbine temperature. This leads to increased blade and vane temperatures and therefore to enhanced oxidation and corrosion attack of the coatings on these components [1]. Such thermal barrier coatings (TBCs) are usually of the MCrAlY type where M is used to represent nickel (Ni), cobalt (Co) or a nickel-cobalt alloy. Besides, the inner surfaces of steel tubular components used for oil, gas, and water pipelines as well as gun tubes and bores usually suffer severe oxidations and corrosions under the conditions of high temperature [2]. The preparation of protective TBCs on inner surfaces of steel tubular components is considered necessary.

Thermal spraying is a convenient processing method permitting a large range of MCrAlY compositions to be obtained [3]. Recently, a more efficient processing method with lower economic cost for fabrication coatings on the metallic surfaces was proposed [4, 5]. Mechanical alloying (MA) is a solid-state processing technique that allows the production of blended powders, homogeneous compounds or alloys. Typically, the MA procedure involves repeated cold welding, fracturing, and re-welding of powder particles in a high-energy ball mill. Meanwhile, the inner surface of the grinding vial is continuously impacted by a number of flying balls and powder particles, resulting in the sticking and deposition of the treated powder on the inner surface. In general, such a phenomenon is regarded undesirable. However, from a contrary view, it is potentially usable to produce coatings on the inner surfaces of ball milling components. Fortunately, MA method, due to its unique working principle, favors the armoring or reinforcing of inner surfaces of metallic tubular components with Ni, Cr, Al, Co and  $\text{Y}_2\text{O}_3$  powder particles that are able to improve the anti-oxidation performance of substrates significantly.

In this work, TBCs of  $\text{NiCrAl}\cdot\text{Y}_2\text{O}_3$  and  $\text{NiCrAlCo}\cdot\text{Y}_2\text{O}_3$  were fabricated on the inner surface of carbon steel tubular components via the high-energy MA method. Material characteristics of the

TBCs were investigated. The high temperature oxidation experiments were carried out to inspect the anti-oxidation properties of the TBCs. According to the analyses of the experimental results and the action mechanisms in the ball-mill vial, the formation mechanisms of the deposited TBCs prepared by the MA method were further detailed in terms of three assumed but reasonable steps.

## Experimental Details

### Apparatus Setup

The Fritsch Pulverisette 6 planetary mono ball-mill used in the present work is showed as Fig.1a. Two  $30 \times 20 \times 5 \text{ mm}^3$  sized components were cut off from the steel wall of the standard 700ml grinding vial (dimensions:  $\Phi 100 \text{ mm}$  inner diameter  $\times 90 \text{ mm}$  height) of the ball mill apparatus (Fig.1b). After that, the substrates could be put into the remained fillisters of the as-cut wall of the ball mill vial. Therefore, one outer surface of the substrate was exposed to the inner grinding vial and contacted with the milling balls and raw powder particles. Aiming to make the powders to be adhered and deposited onto the surface of the substrates, the MA process carried out, and then the interactions between the milling balls, the raw powders and the substrate surfaces succeeded. The further designed mill vial and the unique principle of experimental apparatus are schematically illustrated in Fig.2. The planetary MA apparatus was characterized by the planet-like movement of the grinding vial, which was arranged on a rotating support disk. A precise microprocessor which controlled electronic system drove them to rotate and orbit around their own central axes. Thus, the vial were rotating around its own axis while the support disk orbiting around its own central axis, the centrifugal forces were produced and then exerted on the milling balls and the powders to be ground. Since the supporting disk and the vial rotated in opposite directions, their own centrifugal forces changed directions alternately. Under this condition, the energy developed through the impacts was several times higher than that for conventional ball mills.



Fig.1 Fritsch Pulverisette 6 planetary mono ball-mill (a); illustration of the further designed vial (b).

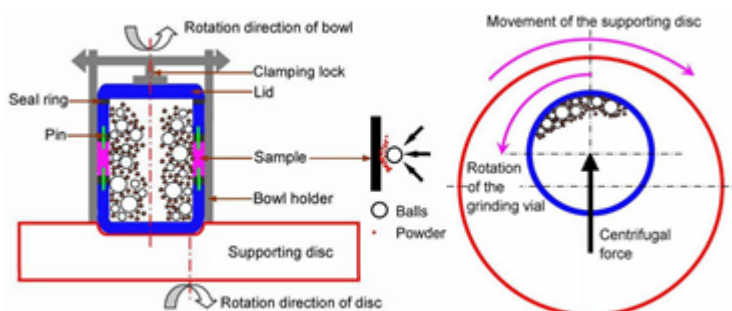


Fig.2 Schematic diagram of preparing coatings by MA technique using the planetary ball-mill.

### Materials

A 45# low carbon steel tubular component to be treated (dimensions:  $\Phi 100 \text{ mm} \times 40 \text{ mm}$ ) was settled in the vial by pins to replace the as-cut component. The Ni, Cr, Al, Co and  $\text{Y}_2\text{O}_3$  powders were used as raw materials for deposition on the inner surfaces of the carbon steel tubular component aiming to obtain  $\text{NiCrAl} \cdot \text{Y}_2\text{O}_3$  and  $\text{NiCrAlCo} \cdot \text{Y}_2\text{O}_3$  coatings. No process control agent was added to the blended powder, and the MA process was carried out in an ambient atmosphere. The weight ratios

of powders before deposition were 66% Ni+17% Cr+5% Al+2%  $Y_2O_3$  for NiCrAl• $Y_2O_3$  coatings and 61% Ni +17% Cr+5% Al+2%  $Y_2O_3$ +5% Co for preparing NiCrAlCo• $Y_2O_3$  coatings. The total weight of every group of blended powders was 30g.

### Processing Parameters

The stainless steel milling balls were charged into the vial: three  $\Phi 20$ mm balls, thirty five  $\Phi 10$ mm balls, and sixty one  $\Phi 6$ mm balls. The gross weight of milling balls was 300g. As a result, the ball-to-powder weight ratios were both 10:1. The MA processes for fabricating TBCs were performed at rotation speeds of 300-500rpm (round per minute) and milling durations of 3-8 h (hour). And the procedure of MA process parameter optimization was not detailed in this paper.

### Microstructural Characterization

Cross-section material characterizations of the coatings were observed and analyzed carefully. Specimens were cut from the as-prepared substrates with coatings using the spark-erosion wire cutting method. Microstructure features were detected by a Quanta200 scanning electron microscope (SEM) with an energy dispersive X-ray spectroscopy (EDX) to examine chemical compositions. Phases of the deposited coatings were identified by a Bruker D8 Advance X-ray diffraction (XRD) analyzer with  $CuK\alpha$  radiation ( $\lambda=0.1540598nm$ ) at 40kV/40mA, using a continuous scan mode.

### Oxidation Testing

The dimensions of specimens for oxidation testing were 10mm×10mm×8mm. The specimens were heated in a constant temperature box type electrical resistance furnace at an operating temperature of 800°C and a holding time of 10h, followed by furnace cooling to the room temperature. The gain in weight of specimens during oxidation testing was measured using a MP1002 electronic balance with a resolution of 0.01g. The specimens were further heated for up to 100h at a regular interval of 10h. The oxidation kinetics curves of the tested coatings were thus monitored by intermittent weight gain measurements repeated 10 times.

## Results and Discussion

### Material Characterization Results

Fig.3 and Fig.4 show the comparison investigation results of the deposited coatings of NiCrAl• $Y_2O_3$  and NiCrAlCo• $Y_2O_3$ , and the MA process parameters were labeled in the figures. It indicated that a proper increase in the applied milling time and the disc rotation speed contributed to the improvement in the thickness, densification level and microstructure homogeneity of the deposited NiCrAl• $Y_2O_3$  and NiCrAlCo• $Y_2O_3$  coatings. On the MA process conditions of 450rpm rotation speed with 8h milling duration, the thickness of TBCs was ~100 $\mu m$ . Aiming to further determine the distributions of main elements, the EDAX line scans were performed along the arrow lines marked in the SEM images of Fig.3b and Fig.4b, from the top coating surfaces to the inner substrates, with the results depicted in Fig.3e and Fig.4e. It shows the linear element distributions of the cross-section of the TBCs produced after milling durations of 8h with rotation speed of 300 rpm. It proved that a thickening procedure of the TBCs occurred after a relatively long milling duration. During the formation process of TBCs, the thin diffusion layers with no more than 5 $\mu m$  thickness were formed on the carbon steel surface.

MA process for material surface treatment can strongly exert influences of surface activation, including generating plastic deformation, producing nanostructured layer and accelerating element diffusion on the as-processed metal surfaces [6, 7]. It made the raw metallic surface to be more activated. The numerous non-equilibrium crystal defects, which were produced by the mechanical treatments of MA process, brought an extra driving force stored on the MA-treating carbon steel surface. Therefore, the steel surface was easier to be diffused and deposited by TBCs powders. The initial diffusion layer had laid a foundation for the following deposition of TBCs. The fresh and

highly activated surfaces were produced continuously, following the thickening procedure of the depositing coatings.

As indicated in Fig.3f and Fig.4f, which were the results of XRD analyses on the  $\text{NiCrAl}\cdot\text{Y}_2\text{O}_3$  and  $\text{NiCrAlCo}\cdot\text{Y}_2\text{O}_3$  TBCs, some kinds of intermetallic compound phases and Ni-based solid solutions were formed in the TBCs prepared by MA process. It was proved that the alloying between the elements had occurred.

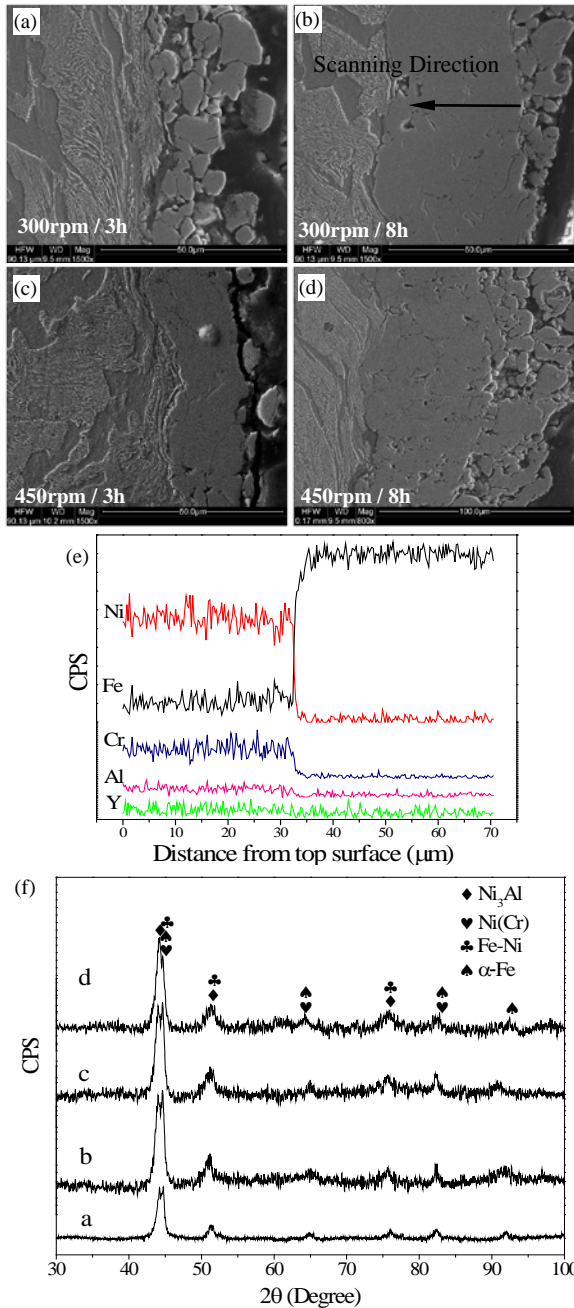


Fig.3 Results of material characterization on  $\text{NiCrAl}\cdot\text{Y}_2\text{O}_3$  coatings: (a)~(d) microstructures of cross-section by SEM; (e) linear distribution of chemical composition in Fig.3b by EDAX; (f) phases of  $\text{NiCrAl}\cdot\text{Y}_2\text{O}_3$  coating by XRD.

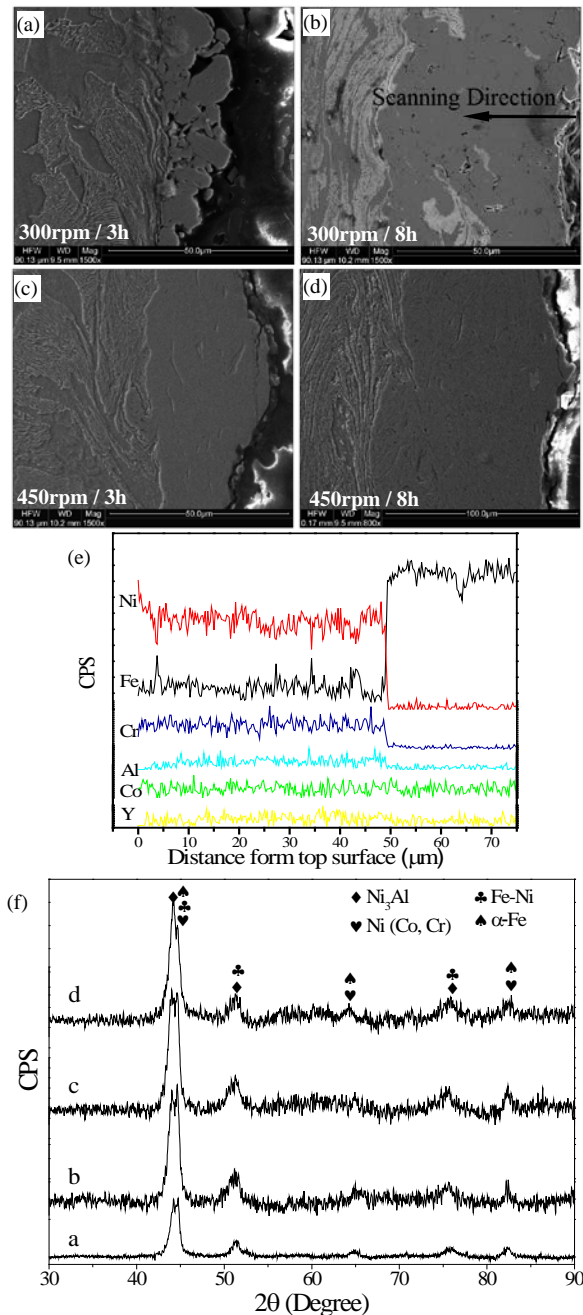


Fig.4 Results of material characterization on  $\text{NiCrAlCo}\cdot\text{Y}_2\text{O}_3$  coatings: (a)~(d) microstructures of cross-section by SEM; (e) linear distribution of chemical composition in Fig.3b by EDAX; (f) phases of  $\text{NiCrAlCo}\cdot\text{Y}_2\text{O}_3$  coating by XRD.

## Formation Mechanism

The above of the present paper and Reference [4, 5] had stated that the planetary ball mill owes its name to the planet-like movement of the grinding vials which are arranged on a rotating support disk, as revealed in Fig.2. By comparison, at the same milling duration, the energy input into milling balls and powders within the planetary ball-mill is much higher than that within the conventional ball-mills

[8]. And the temperature inner the milling vial after heating-up is higher than that during other process method of surface mechanical treatments, such as shot-peen [8]. In the MA apparatus of this experimental work, the centrifugal forces are thus produced by the vials rotating around their own axes, and the support disk orbiting around the central axis. The centrifugal forces are then exerted on the grinding balls, powder particles and metallic surfaces of tubular components to be ground. Since the vials and the supporting disk rotate in opposite directions, the centrifugal forces alternately change their directions. Under this condition, the grinding balls are primarily carried up the inner surface of the carbon steel tubular components and then run down along the inside wall, producing a so-called ‘friction effect’ on the inner surface of the tube components. Subsequently, the grinding balls and the materials being ground are propelled off the inner wall and travel freely across the inner chamber of the vial, colliding against the opposite inside wall and the inner surface of tubular components. In this situation, another new mechanism, a so-called ‘impact effect’, is developed during the interaction. The energy developed through the impacts is several times higher than that for conventional ball mills. Therefore, the inner metallic substrate tends to undergo a higher rate of plastic deformation, thereby increasing their surface activity significantly. The highly activated surface state makes the adherence of powders to be easier. In addition, a larger macroscopic temperature rise of the vial can provide a thermo-dynamical condition for the diffusion alloying in the deposited coatings.

It is assumed that the deposited coatings within the in-situ intermetallic phases and solid solutions on the surface of the carbon steel substrates by means of the following three steps, which are schematically illustrated in Fig.5.

(i) Due to the repeated collision between the milling balls and the inner wall, the substrate surface suffers a large degree of plastic deformation and then starts to become activated. A fraction of TBCs blended powders, especially the hard ceramic particles of  $Y_2O_3$ , are easy to transfer and adhere onto such an activated substrate inner surface. The non-equilibrium lattice defects produced by the repeated collisions bring an extra driving force stored on the substrate surface. And the hard ceramic particles of  $Y_2O_3$  are embedded into the plastic surface layer due to the ‘hammer-into’ mechanism. It is different from the plastic metallic powder particles.

(ii) The further ball-to-substrate collisions make more and more adhered powders of Ni/Cr/Al and hard ceramic particles of  $Y_2O_3$  to be hammered together on the highly activated substrate surface through the repeated action of cold-welding. Thus, a coating layer is formed. Meanwhile, the diffusion of Fe, Ni, Cr, Al and Co atoms is initiated to transform a thin diffusion layer between the steel substrate and the interior wall of coating. Then, the diffusion layer initially transforms to a coating/substrate interface region.

(iii) After prolonging the milling duration or accelerating the rotation speed of MA apparatus, the sufficient inter-diffusion, alloying reaction and/or solid solution between the individual elements of Fe/Ni/Cr/Al/Co occurs. And more powders are flattened, cold-welded, and deposited on the newly present and activated layer due to continuous ball collisions, leading to an outward growth and thickening of the  $NiCrAl \cdot Y_2O_3$  and  $NiCrAlCo \cdot Y_2O_3$  coatings. The final thickness of TBCs is strongly related to the adhesivity of the raw metal powders.

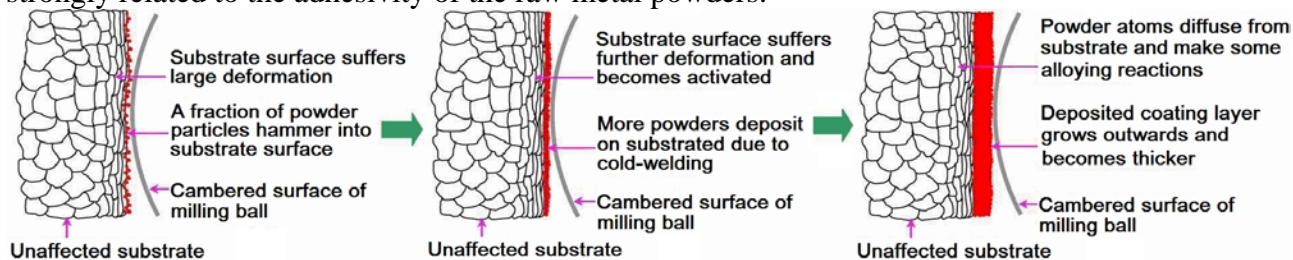


Fig.5 Schematic of formation mechanisms of the deposited coating prepared by MA process.

## Oxidation Testing Results and Analysis

Fig.6 shows the oxidation weight gains of carbon steel substrates with and without MA-processed TBCs treated up to 100h at 800°C. It showed that the oxidation rate of the substrate with



NiCrAlCo•Y<sub>2</sub>O<sub>3</sub> was significantly lower than both of that without a protective coating and that with NiCrAl•Y<sub>2</sub>O<sub>3</sub>. As stated above, the thickness of the TBCs prepared by MA was increased with both the acceleration of MA apparatus rotation and the extension of milling duration. As depicted in Fig.6, the thicker TBCs contributed to the anti-oxidation property more effectively. On the process condition of 450rpm/8h, the weight gain of the substrate with NiCrAlCo•Y<sub>2</sub>O<sub>3</sub> coating was 629.5mg/cm<sup>2</sup> after 100h treatment. Fig.7 gives the surface appearances of the as-treated carbon steel substrates without or with the TBCs prepared by the MA process. It indicates that the addition of Co trace element in the NiCrAl•Y<sub>2</sub>O<sub>3</sub> coating significantly enhances its anti-oxidation capability.

Reference [9, 10] had stated that the oxidation protective layers of NiO, Cr<sub>2</sub>O<sub>3</sub> and Al<sub>2</sub>O<sub>3</sub> were formed during the heat-treated testing in the environment of 1000°C high temperature. Furthermore, the following chemical reaction could occur when the contain of Cr was enough, as in



Thus, the continuous formation of Cr<sub>2</sub>O<sub>3</sub> surface oxide film reduces the oxygen activity at the interface of oxide and metal, so that the aluminum, which is even at a low concentration, can continuously produce the selective oxidation of Al<sub>2</sub>O<sub>3</sub> oxide film.

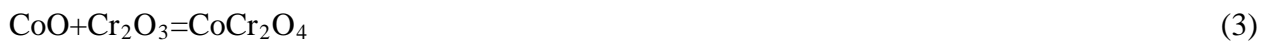
At high temperature and high pressure, the Cr<sub>2</sub>O<sub>3</sub> oxide will gradually evaporate as the form of CrO<sub>3</sub>, leaving a continuously protective oxide film of Al<sub>2</sub>O<sub>3</sub>. During the transition stage of oxidation, the oxide film composition gradually changes. The formation of Cr<sub>2</sub>O<sub>3</sub> intermediates plays a role in preventing the oxidation of aluminum.

In addition, the process of alloying elements to generate oxide are strongly related to their chemical stability, as in

$$\frac{1}{3}\Delta G^\circ(\text{Al}_2\text{O}_3) < \frac{1}{3}\Delta G^\circ(\text{Cr}_2\text{O}_3) < \frac{1}{3}\Delta G^\circ(\text{NiO}) \quad (2)$$

Therefore, Al<sub>2</sub>O<sub>3</sub> is the most stable oxide, and the most unstable oxide is NiO. Adding a neutral element between the binary alloy elements will reduce the partial oxygen pressure of the selective oxides of the most active element. And those can promote the selective oxidation of the most stable element.

The element of Co played an important role in the anti-oxidation testing. The main reactions are as follows.



In the oxidation process, these CoCr<sub>2</sub>O<sub>4</sub> and CoAl<sub>2</sub>O<sub>4</sub> typed oxides were generated by reactions of metal ions and retarded the diffusion of metal ions. And the effect of retardation by CoCr<sub>2</sub>O<sub>4</sub> and CoAl<sub>2</sub>O<sub>4</sub> was more efficient than that by CoO, Cr<sub>2</sub>O<sub>3</sub> and Al<sub>2</sub>O<sub>3</sub>.

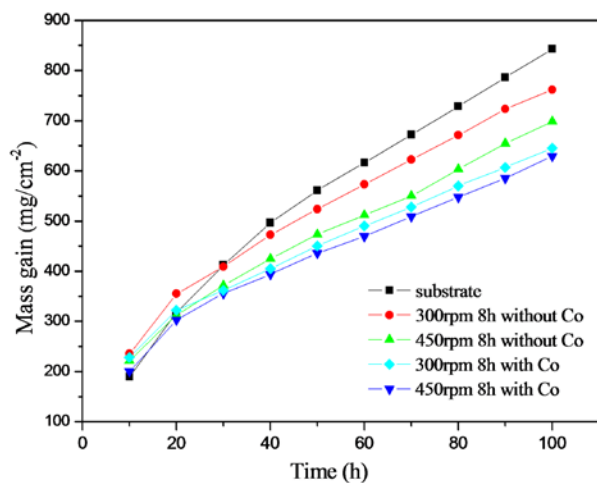


Fig.6 Oxidation weight gains at 800 °C to 100h for inner substrates with and without mechanically alloyed TBCs (NiCrAl•Y<sub>2</sub>O<sub>3</sub> and NiCrAlCo•Y<sub>2</sub>O<sub>3</sub>).

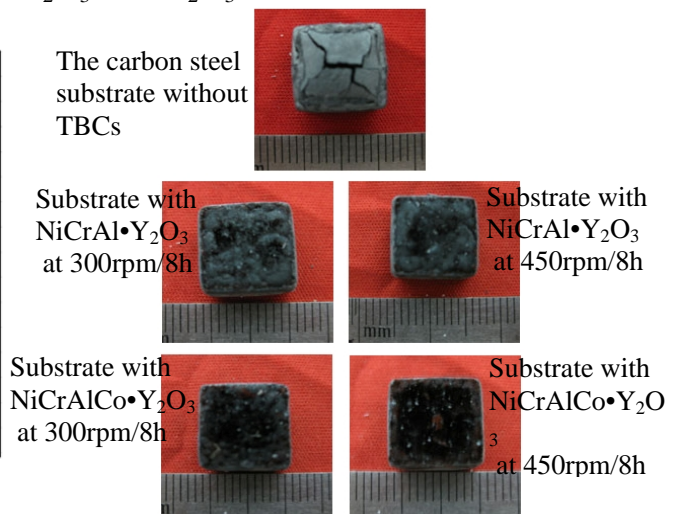


Fig.7 Oxidation appearances of the as-treated samples without or with the TBCs (NiCrAl•Y<sub>2</sub>O<sub>3</sub> and NiCrAlCo•Y<sub>2</sub>O<sub>3</sub>).

## Acknowledgment

The work was supported by the National Natural Science Foundation of China (Grant No.51505293) and China Postdoctoral Science Foundation funded project (2015M580342).

## References

- [1] S. Sanaye, A. Fardad, and M. Mostakhdemi: *Energy.*, Vol. 36 (2011), p. 1057-1067
- [2] Z. Zhan, Y. He, D. Wang, and W. Gao: *Surf. Coat. Tech.*, Vol. 201 (2006), p. 2684-2689
- [3] L. Pawlowski: *The science and engineering of thermal spray coatings* (Wiley, New York 2008)
- [4] D. Gu and Y. Shen: *Appl. Surf. Sci.*, Vol. 256 (2009), p. 223-230
- [5] B. Li, R. Ding, Y. Shen, Y. Hu, and Y. Guo: *Mater. Des.*, Vol. 35 (2012), p. 25-36
- [6] I. Farahbakhsh, A. Zakeri, P. Manikandan, and K. Hokamoto: *Appl. Surf. Sci.*, Vol. 257 (2012), p. 2830-2837
- [7] G. Gupta, K. Mondal, and R. Balasubramaniam: *J. Alloy. Compd.* Vol. 482 (2009), p. 118-122
- [8] C. Suryanarayana: *Prog. Mater. Sci.*, Vol. 46 (2001), p. 1-184
- [9] C. Giggins and F. Pettit: *J. Electrochem. Soc.*, Vol. 118 (1971), p. 1782
- [10] C. Wagner: *J. Electrochem. Soc.*, Vol. 103 (1956), p. 571